

An Alternative Approach in Power Line Communication Channel Modelling

Fulatsa Zwane* and Thomas J. O. Afullo

Abstract—In this paper, we present the measurement methodology and results for a low voltage Power line Communications (PLC) network under different configurations. Based on the measurements, a correlation of the channel transfer characteristics to the network topology is established and a deterministic model based on two-wire transmission line theory for transverse electromagnetic (TEM) wave propagation is proposed. The channel frequency response in frequency range of 1–30 MHz is determined, where the model results agree well with the measurements.

1. INTRODUCTION

The development of accurate power line communication (PLC) channel transfer characteristics models is important as it forms the basis for computer simulations which are useful in appropriate system design, and further enable the analysis of the performance of different network configurations and loads [1]. There is therefore continued research in the characterization of the power line as a communication medium. Different techniques which are based on either measurements or theoretical derivations from physical parameters, denoted as top-down or empirical models [2, 3], and bottom-up or deterministic models [4–6], respectively, are employed. The empirical model is easy to use as it calls for little computation and is easy to implement. It is however susceptible to measurement errors and cannot be used to reproduce the channel characteristics of a different PLC network. The deterministic model differs from the latter in that it necessitates detailed knowledge of all components and their respective characteristics. Therefore the network behaviour in relation to the model parameters is clearly defined, and is considered in this work.

True to its original purpose, the low voltage power line network within a typical in-building structure is optimized for the transmission of high voltages at low frequencies contrary to data transmission which necessitates the transmission of low voltage at high frequencies. The communication signals therefore suffer some hostile channel parameters. The three most important parameters are noise, impedance mismatch, and attenuation which are frequency, time and location variant [7].

Subsequently, accurate approximation of the line parameters, the characteristic impedance Z_0 , and propagation constant γ , which in turn are used to determine the PLC channel constants, is essential in the channel transfer function calculations. Meticulous measurements are required in the investigation of the channel parameters and consequent modelling of the same. The behaviour of the channel is better understood by varying different components, which in the case of PLC, are: the topology; the cable types; the cable length and number of branches; as well as the loads terminating at each end of the network. Once relations of the variations of these are obtained, any given network can then be sufficiently modelled.

Received 13 December 2013, Accepted 29 January 2014, Scheduled 3 February 2014

* Corresponding author: Fulatsa Zwane (211560595@stu.ukzn.ac.za).

The authors are with the Department of Electrical, Electronic and Computer Engineering, University of KwaZulu-Natal, Private Bag X54001, Durban 4001, South Africa.

The work presented here seeks to contribute to the on-going research of developing a better understanding of the medium. The test bed set up, extraction and measurement results of the line parameters and channel frequency response for different configurations are discussed in Section 2. In Section 3, we present the proposed model and analytical results. The conclusions are then drawn in Section 4.

2. MEASUREMENT METHODOLOGY

2.1. Line Parameter Measurement

The characteristics of the cable forming the network, the Cu $3 \times 2.5 \text{ mm}^2$ Cabtyre flexible PVC cables measured are shown in Figs. 1(a) and 1(b), that is, the characteristic impedance and attenuation constant respectively. Theoretically, from the two conductor transmission line model, the differential length Δx of the transmission line is described by the distributed parameters, R' , the resistance per unit length, L' , the inductance per unit length, G' , the conductance and C' , the capacitance per unit length. The characteristic impedance is calculated as [8]:

$$Z_0 = \sqrt{\frac{R' + j\omega L'}{G' + j\omega C'}} \quad (1)$$

The propagation constant calculated as [8]:

$$\gamma = \sqrt{(R' + j\omega L')(G' + j\omega C')} = \alpha + j\beta \quad (2)$$

where α = the attenuation constant in Np/m, β = the phase constant in rad/m.

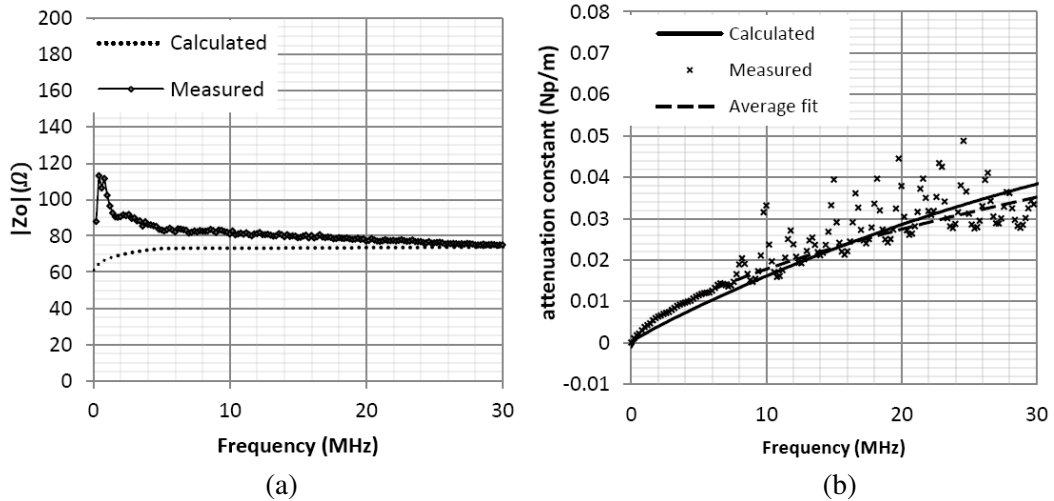


Figure 1. (a) The characteristic impedance for the 2.5 mm^2 transmission line. (b) The measured and calculated attenuation coefficient for the 2.5 mm^2 cable.

Experimentally, they are obtained from the measurement of the input impedance of short circuit ended and open circuit ended cables using the ZVL Rohde & Schwarz Vector Network Analyzer as [9]:

$$Z_0 = \sqrt{Z_{sc} Z_{oc}} \quad (3)$$

$$\gamma = \frac{1}{l} \tanh^{-1} \sqrt{\frac{Z_{sc}}{Z_{oc}}} \quad (4)$$

where l = cable length, Z_{oc} = input impedance of open circuited cable end and Z_{sc} = input impedance of short circuited cable end.

2.2. Channel Frequency Response Measurements

The measurement setup consists of a ZVL Rohde & Shwarz Vector Network Analyzer connected to the power line channel at both transmitting and receiving ends via couplers. A differential mode based passive coupling circuitry has been designed to couple the communication signals onto and from the power line. One terminal is connected to the live conductor (L) and the other to the neutral conductor (N). A high voltage capacitor is used due its capacity to block the 50 Hz, 230 V low voltage power line signals, also preventing the saturation of the coupling transformer [10].

Between the communication and power line circuitry, the transformer offers galvanic isolation and acts as a limiter [11]. Extra protective circuitry is included to the coupler design; the back to back zener diodes are included to limit the output level as well as grip fast transient disturbances. A metal oxide varistor (MOV) is included for surge protection through its capability to limit over voltage spikes, therefore avoiding damage to the capacitor. The transfer function and design of the coupler used to interface the measuring equipment to the power line is as depicted in Fig. 2.

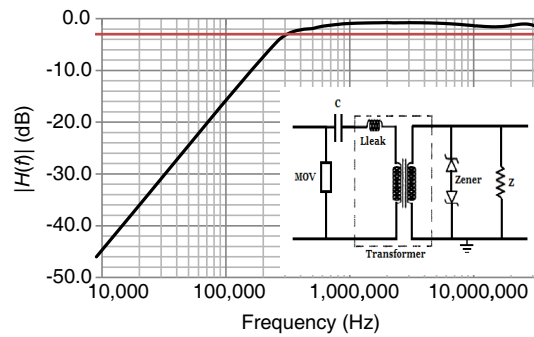


Figure 2. The coupler design and transfer function.

An alternative measuring setup, given a network with the input and output ports separated by a large distance would be to employ a calibrated signal generator and measuring equipment on the different ends. Here, the measured data may be stored and processed on a computer. Again, couplers designed as discussed above are to be connected to the equipment for protection.

To meaningfully explore the characteristics of the PLC channel measurements for different topologies and variations are done as follows, where in all measurements, unless stated, the branch terminals are open circuit ended:

- a. The live network with a T-node topology as depicted in Fig. 3(a) is tested and the frequency response for different configurations, that is, for different test points are measured according to configurations stated in Table 1. The transfer function is shown in Fig. 3(b) where the least squares method is used and the logarithmic regression estimates are determined to find the average path loss. Fig. 3(c) shows the phase response of the same configurations. The transfer function is seen to have notches at different frequency points which correspond to the distortions in the phase response.
- b. Measurements were also taken for a two T-node network as shown in Fig. 4(a) and the transfer function for two different configurations shown in Fig. 4(b). Fig. 4(c) shows the phase response of the relevant configurations.

Table 1. The different configurations for the two networks.

		Transmit	Receive
Network 1	Config.1	(1)	(3)
	Config.2	(1)	(2)
Network 2	Config.3	(1)	(3)
	Config.4	(1)	(4)

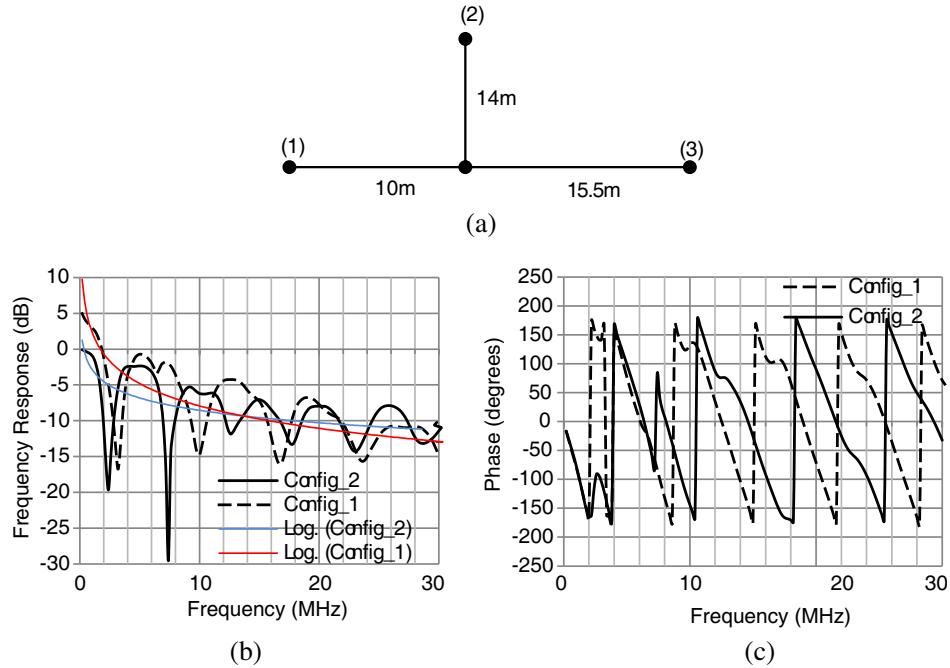


Figure 3. (a) The T node topology. (b) The transfer function for different configurations of the T node topology. (c) The phase response for different configurations of the T node topology.

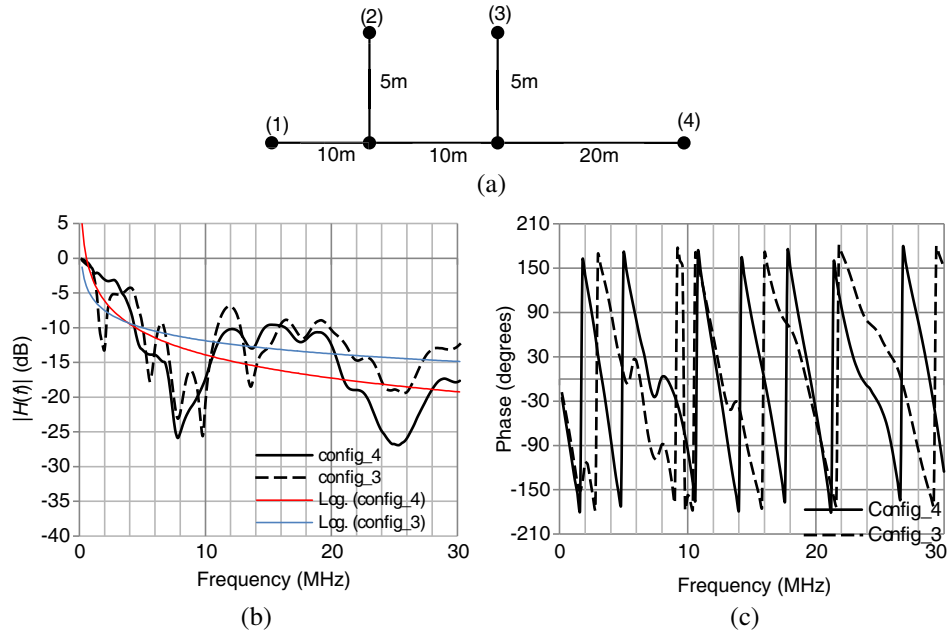


Figure 4. (a) Illustration of a two T-node topology. (b) The transfer function for two configurations of the two T-node topology. (c) The phase response for two configurations of the two T-node topology.

- c. The two networks were cascaded to form a three T node network topology as shown in Fig. 5(a) with the measured channel frequency response, labeled as Config_5 as shown in Fig. 5(b). This is plotted against the transfer function obtained from adding the single T-node (Config.1) to the two T-node topology (Config_4), labeled as Cascade 1 and 4.
- d. The T-node with a topology as in Config.2 was measured with the branch termination open circuited and closed circuited has the channel transfer function results as shown in Fig. 6.

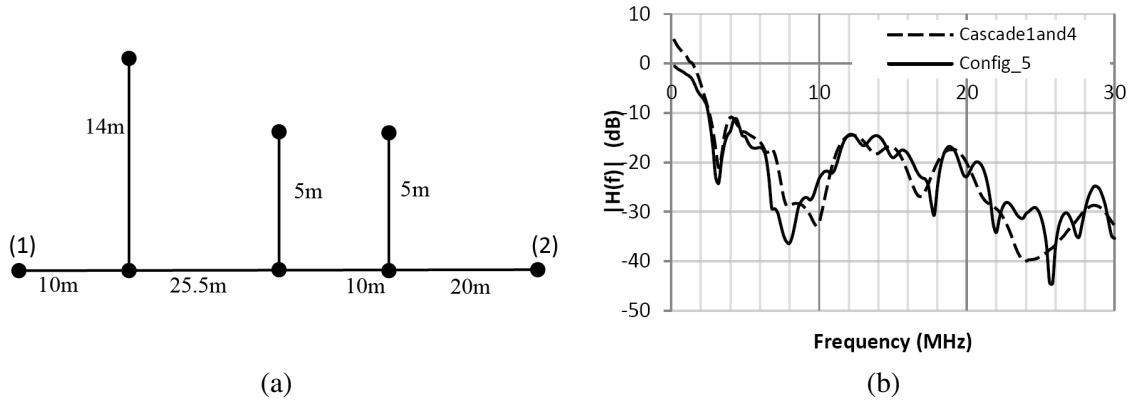


Figure 5. (a) The three T-node network. (b) Transfer function of the two networks cascade.

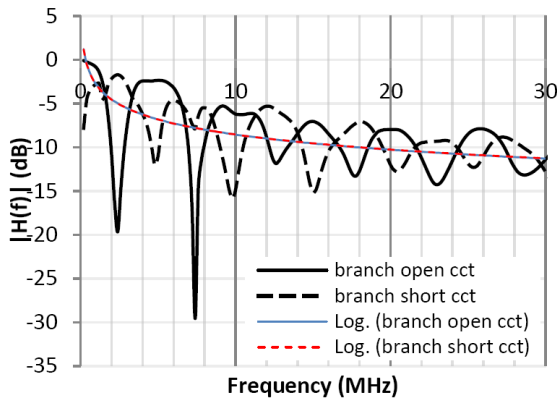


Figure 6. The transfer function for a T-node with branch end short circuited and open circuited.

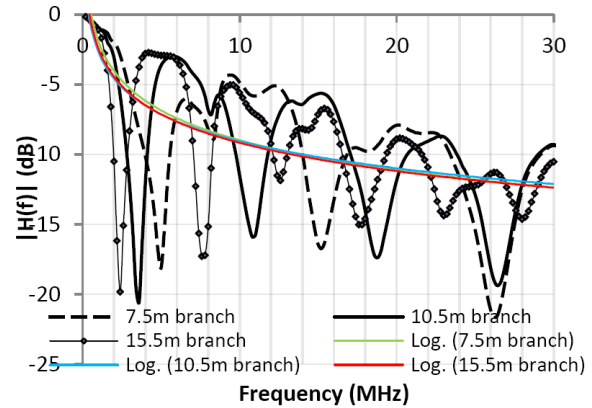


Figure 7. Measurement results for variation in branch length of the same network.

e. Figure 7 shows the channel transfer function for the different branch lengths of the T-node topology as in Network 1 measured for different branch lengths (7.5 m, 10.5 m 15.5 m).

2.3. Discussion of Results

From the measurements we are therefore able to deduce the following characteristics of the PLC channel:

a. Notch separation and position: The transfer functions have notches at different points. A trend can be seen in the notches occurrence, the separation between the notches is seen to be equal. We consider the electric length of the branch expressed in units of the wavelength λ , related to the propagation velocity v_p and signal frequency f by [12]:

$$\lambda = \frac{v_p}{f} \tag{5}$$

As the impedance of the channel is frequency dependent, for the open circuit end, the first notch will occur at a resonant frequency, relative to the length of the branch, which we shall refer to as d , and propagation velocity v_p , related by:

$$f_0 = \frac{v_p}{4d} \tag{6}$$

From the measurements the propagation velocity was estimated to be 1.488×10^8 . Given the first notch of the open circuit ended branch termination, solving for d will give a value of 15.5 m.

The subsequent notches will be at frequencies given by:

$$f_{ok} = \frac{v_p}{4d}(2k + 1), \quad k = 1, 2, \dots \quad (7)$$

For the short circuited branch termination the notch will occur first at zero and then at the frequencies given by:

$$f_{sk} = \frac{v_p}{4d}(2k), \quad k = 1, 2, \dots \quad (8)$$

Therefore if the branch length is known, we will be able to determine the notch positions and separation for the open circuited and short circuited branch terminations. Moreover having a reference branch length, varying the length by a factor n will give a resulting first notch at frequency:

$$f'_0 = \frac{1}{n}f_0 \quad (9)$$

- b. Cascade of networks: The measured transfer function for the three-branch network follows the same trend as the one obtained from the adding that of config_1 and config_4. The variations are due to the difference in impedance at the cascade point, instead of a receiver termination of 50Ω for network 1 and transmitter input impedance of 50Ω for network 2, the cables are joined to form a straight connection from the same cable type. This, however, has shown that the transfer function can be calculated as cascaded elements as:

$$H_{total}(\text{dB}) = H_{config_1}(\text{dB}) + H_{config_2}(\text{dB}) \quad (10)$$

- c. Relation to direct path length: Although there is a marginal difference in the average path loss for the first two configurations, the gradient is seen to be larger with the increase in the distance from the transmitting end to the receiving end, this is clearly shown in Fig. 4(b). From Figs. 6 and 7 the average path loss is the same, as the distance from transmitter to receiver is the same, given different branch loads and branch lengths. This shows that the distance forming the direct path from the transmitter to receiver is the average attenuation path determinant by a factor A . In theory, if we consider a transmission line of length l and excited by a sinusoidal AC generator at the other end, the voltage phasors at these positions are related as [8]:

$$H(f) = \frac{V(l)}{V(0)} = e^{-\gamma l} \quad (11)$$

where γ = the propagation constant as seen in (2), to have the attenuation and phase constant. The average attenuation path determinant A , therefore can be seen as:

$$A(f, l) = e^{-al} \quad (12)$$

where a = the attenuation constant of the power line from the propagation constant and l = the direct path from transmitter to receiver.

3. PROPOSED MODEL

The power line is described as a cascade of series resonant circuits (SRC) by [3], where one series resonant circuit connected to a line with impedance Z is represented as in Fig. 8(a).

The impedance of the frequency dependent resonant circuit Z_S is described by:

$$Z_S = R + j \cdot 2\pi f \cdot L + \frac{1}{j \cdot 2\pi f \cdot C} \quad (13)$$

where R = the series resistance, L = the series inductance and C = the series capacitance.

The transfer function for each resonant circuit is given by:

$$Hr(f) = \frac{Z_S(f)}{Z_S(f) + Z} \quad (14)$$

where Z = the line impedance.

An evolutionary strategy is employed by [3] to determine the optimized component parameters of the SRC. The model by [13] uses the two conductor transmission line theory unit length parameters.

When considering measurement results shown by various literature and in the above section, the transfer function can be viewed as a cascade of the amplitude response for a single SRC, with different resonant frequencies following a certain gradient.

From measurements in the Section above, we obtained the correlation of the notches to the branch properties. As the PLC channel is time and frequency variant, tracking the load impedances at multiple branch terminals is cumbersome. To serve as a general reference channel model for a network of the same cable parameters, this proposed model will help in the design and development of PLC communication systems by considering the extreme cases, that is, the short circuit and open circuit branch termination impedances. The characteristic impedance of the cable is assumed to be the uniform and the source and load impedances at transmitter and receiver respectively are known.

The transmission line theory for short circuited and open circuited ends is employed. By analysing the input impedance characteristics around a resonant wavelength λ_r , circuits in Fig. 9(a) and Fig. 9(b) behave like a series RLC circuit [14]. We take Fig. 8(a) therefore to represent our equivalent circuit for the branch line as in Fig. 8(b).

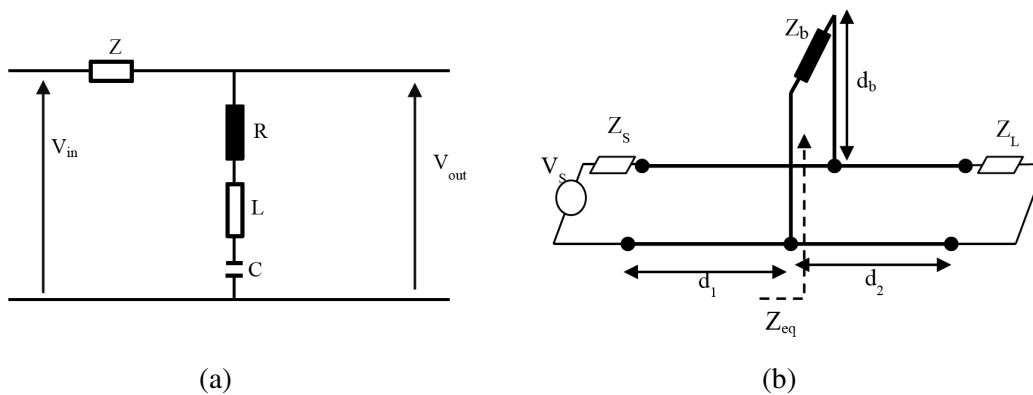


Figure 8. (a) The series resonant circuit. (b) The T-node topology connected to source and load.

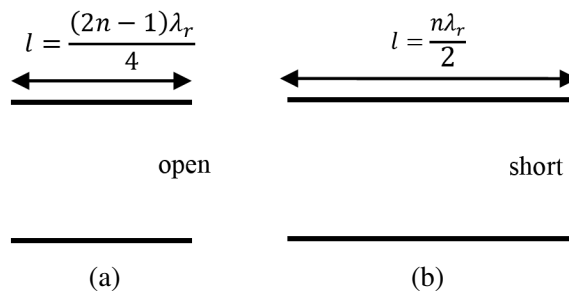


Figure 9. Types of transmission line series resonant circuits with length (a) a quarter wavelength and (b) a half wavelength.

For the open circuited end, the length of the cable is in odd multiples of $\lambda_r/4$ and for the short circuited end, the length of the cable is in even multiples of $\lambda_r/2$. Table 2 gives the determination of the series RLC parameters [14].

Each resonant circuit is described by a transfer function $Hr_i(f)$ and the overall transfer function is given as:

$$H(f) = A \prod_{i=1}^n Hr_i(f) \tag{15}$$

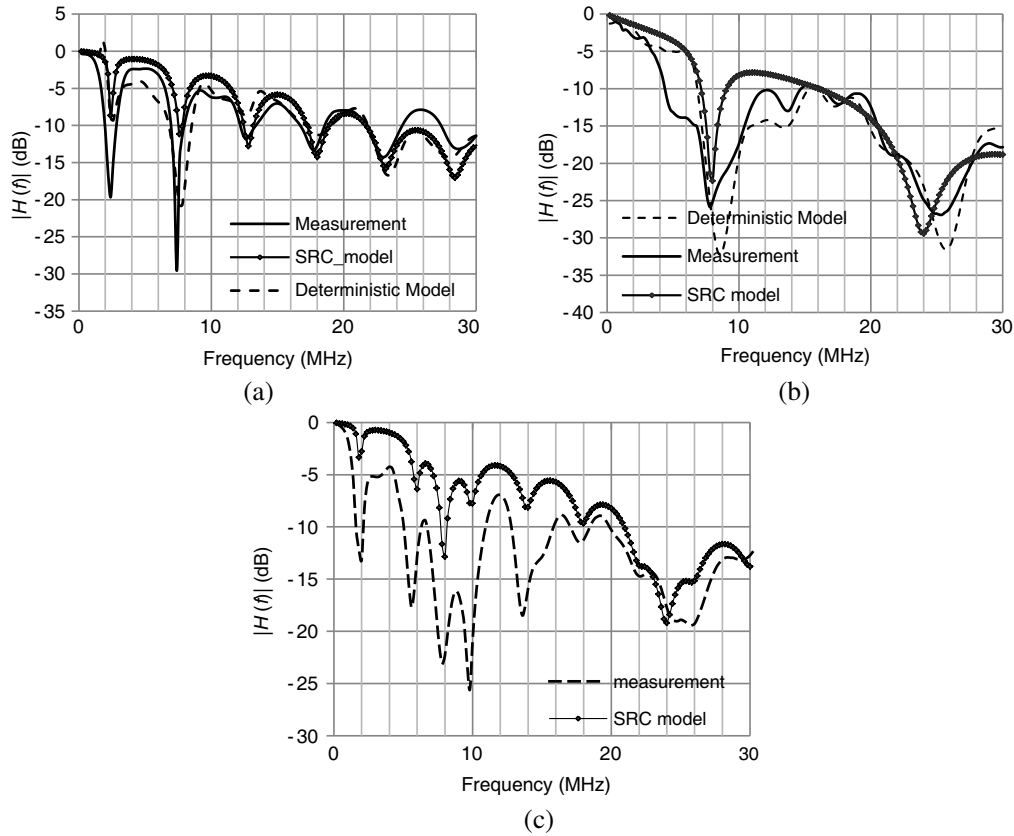
where n = the number of series resonant circuits forming the total transfer function and A = the average path loss factor, as derived in (12) with the length l determined by the transmitter to receiver distance.

Table 2. Series resonance RLC parameters.

Resonance	Quarter wavelength ($\lambda_r/4$)	Half wavelength ($\lambda_r/2$)
	Open circuit	Short circuit
R	$\frac{1}{4}Z_0\alpha\lambda_r$	$\frac{1}{2}Z_0\alpha\lambda_r$
L	$\frac{\pi Z_0}{4\cdot\omega_0}$	$\frac{\pi Z_0}{2\cdot\omega_0}$
C	$\frac{4}{\pi\omega_0 Z_0}$	$\frac{2}{\pi\omega_0 Z_0}$
Q	$\frac{\beta_r}{2\alpha}$	$\frac{\beta_r}{2\alpha}$

where Z_0 = the characteristic impedance of the line, ω_0 = the resonant angular frequency, α = the attenuation constant of the line, λ_r = the wavelength at resonance and $\beta_r = \pi/l$.

The model proposed herein is compared to measurements as well as the model by [4], obtained for Config_2 and Config_4 as shown in Figs. 10(a) and 10(b) respectively. The model transfer function follows that of the actual measurements. It shows that an estimate of the transfer function for a channel with an open circuited branch end can be produced from the knowledge of the branch length, characteristic impedance and attenuation constant. In Fig. 10(c), Config_3 is considered. The notch positions are seen to be replicated by the calculation of branch transfer function with a notable deviation in the average path loss at certain frequencies.

**Figure 10.** The measurements of (a) a single T-node, (b) the two T-node topology and (c) the three T-node topology compared to the SRC model analytical results.

4. CONCLUSIONS

In this paper, we examine the characteristics of the PLC channel. The measurement methodology is discussed and the channel frequency response results are shown. The channel characteristics are seen to be dependent on length, load and power line characteristics. The notches in the transfer function are seen to be determined by the branch length and a relation to this effect is formed for short circuited and open circuited branch terminations. A SRC model is proposed following the characteristics of the PLC channel. The model results compared to measurements as well as a deterministic model by [4] demonstrate the accuracy of the model applied to actual networks.

Given the principles followed in formulating the model, the results shown in the different presented figures and the principle established in the cascade of networks, a large deviation for more complex networks is not anticipated. When considering the deviations in the average path loss, they seem disadvantageous. However, essential effects given the applicability of the model to actual networks, for simulation based PLC system performance applications have been covered. Further investigations on the deviation cases by exploring more complex networks are being done.

REFERENCES

1. Róka, R. and S. Dlhá, "Modeling of transmission channels over the low-voltage power distribution network," *Journal of Electrical Engineering*, Vol. 56, Nos. 9–10, 237–245, 2005.
2. Zimmermann, M. and K. Dostert, "A multi-path signal propagation model for the power line channel in the high frequency range," *Proc. Int. Symp. Power Line Communications and Its Applic. (ISPLC 1999)*, 45–51, 1999.
3. Philipps, H., "Modelling of powerline communication channels," *Intl. Symposium on Power-line Communication and Its Applications*, 2005.
4. Meng, H., S. Chen, Y. L. Guan, C. L. Law, P. L. So, E. Gunawan, and T. T. Lie, "A transmission line model for high-frequency power line communication channel," *Proc. 5th Int. Conf. Power System Technology (PowerCon 2002)*, 1290–1295, 2002.
5. Esmailian, T., F. Kschischang, and G. Gulak, "An in-building power line channel simulator," *Proc. Int. Symp. Power Line Communication and Its Applic.*, 1–5, Greece, 2002.
6. Anatory, J., M. M. Kissaka, and N. H. Mvungi, "Channel model for broadband powerline communication," *IEEE Trans. on Power Delivery*, Vol. 22, No. 1, 135–141, 2007.
7. Philipps, H., "Performance measurements of power-line channels at high frequencies," *Proceedings of the International Symposium on Power Line Communications and Its Applications (ISPLC)*, 229–237, 1998.
8. Pozar, D. M., *Microwave Engineering*, 4th Edition, Wiley, New York, 2012.
9. Gianaroli, F., A. Barbieri, F. Pancaldi, A. Mazzanti, and G. M. Vitetta, "A novel approach to power-line channel modeling," *IEEE Transactions on Power Delivery*, Vol. 25, No. 1, 132–140, 2010.
10. Janse van Rensburg, P. A. and H. C. Ferreira, "Coupling circuitry: Understanding the functions of different components," *Proc. 7th Int. Symp. Power-line Comm.*, 204–209, 2003.
11. Janse van Rensburg, P. A. and H. C. Ferreira, "The role of magnetizing and leakage inductance in transformer coupling circuitry," *Proc. 8th Int. Symp. Power-line Comm.*, 244–249, 2004.
12. Smith, A., *Radio Frequency Principles and Applications: The Generation, Propagation, and Reception of Signals and Noise*, Wiley-IEEE Press, 1998.
13. Mulangu, C. T., T. J. Afullo, and N. M. Ijumba, "Modelling of broadband powerline communication channels," *SAIEE*, Vol. 102, No. 4, Dec. 2011.
14. Misra, D., *Radio-frequency and Microwave Communication Circuits: Analysis and Design*, John Wiley & Sons, 2001.